Laser intensity stabilization control for an atomic spin gyroscope

Li Xing, Zhuo Wang*, Jiong Huang, Wei Quan, Wenfeng Fan and Liwei Jiang
School of Instrumentation Science and Opto-electronics Engineering, Key Laboratory of Ministry of Industry and Information Technology on Quantum Sensing Technology, Beihang University
Beijing 100191, China
* Corresponding author, E-mail: zwang8381@foxmail.com

***Abstract*—The stability of laser intensity has important significance for a spin-exchange-relaxation-free (SERF) atomic spin gyroscope. The fluctuation of pump-beam intensity results in the instability of the spin polarization. The background noise level is greatly influenced by the probe-beam intensity stability. In this paper, a liquid crystal variable retarder (LCVR) based laser intensity stabilization control system has been designed for a SERF atomic gyroscope. The probe-beam optical path is composed of two parallel linear polarizers, a LCVR, a photoelastic modulator (PEM) module, a non-polarizing beam splitter (NPBS) and a photodiode. A small fraction of laser intensity is split by the NPBS and detected by the photodiode. Then the signal is fed into the electronic control unit (ECU), which can generate a control signal by the digital controller and drive the LCVR to control the laser intensity. The pump-beam intensity is controlled by the fundamental component of LCVR module. In our experiments, the long-term stability of the laser intensity achieves 0.0084% (of the standard deviation) in a 4-hour measurement. This method can effectively shorten the optical path and improve the stability of our gyroscope.**

Keywords—SERF atomic gyroscope; Laser intensity stabilization control; LCVR module; PEM module

I. INTRODUCTION

Ultra-high precision gyroscopes have found applications in inertial navigation for satellites, airplanes, submarines, ships, etc. [1, 2]. With the development of quantum mechanics and modern optics, atomic spin gyroscope (ASG) has emerged in recent years, which could be used in any applications requiring high sensitivity inertial navigation, portability and low cost. Moreover, the ASG, which is based on an alkali-metal-noble-gas comagnetometer, operates in the SERF regime where the spin exchange relaxation rate is much larger than the Larmor precession frequency to improve the sensitivity limit [3]. The first SERF atomic spin gyroscope was designed by M.V. Romalis et al. in 2005, which achieved angle random walk (ARW) of 0.002 deg/h$^{1/2}$ and long-term stability of 0.04 deg/h with a K-^{3}He comagnetometer [4].

In the SERF ASG, the polarized noble gas can effectively decrease the sensitivity to the magnetic fields, but the ability to achieve ultra-sensitivity rotation measurements has been maintained [5]. However, several measures should be implemented to further suppress the long-term drifts. The SERF ASGs are mainly consist of the optical system, vapor cell system, magnetic shields and magnetic compensation system [6]. Here, we analyze the effect of laser intensity fluctuation on the SERF ASG by coupling the Bloch equations, and suppress the fluctuation by using a LCVR control system. The LCVR [7, 8] has enormous advantages benefiting from its miniaturization, low operation voltage and easy combination of light path. In our experimental apparatus, the LCVR control system is combined with a PEM module [9] to suppress the 1/f noise at low frequencies. The laser intensity closed-loop control covers the whole optical path of the ASG prototype to insure the laser stability before passing through the cell. Finally, the stability of 0.0084% (of the standard deviation) in a 4-hour test is achieved by optimizing the light path and electronic control unit, and the background noise of the SERF ASG is significantly reduced.

A laser intensity stabilization control system based on LCVR for a SERF ASG is proposed in this paper. In Section 2, the effect of pump-beam intensity fluctuation is analyzed through the Bloch equations and the variation of intensity is obtained from the Jones matrices. In Section 3, the experiment setup, a SERF ASG and the LCVR electronic control unit are demonstrated. In Section 4, the experimental results of the laser intensity stability for our gyroscope are shown.

II. PRINCIPLES

A. The effect of laser intensity fluctuation

The dynamics of the SERF ASG can be described by the following Bloch equations [3, 10]:

$$\frac{\partial \mathbf{P}^e}{\partial t} = \frac{\gamma^e}{Q(P^e)}(\mathbf{B}+\mathbf{B}_n+\mathbf{L})\times\mathbf{P}^e - \mathbf{\Omega}\times\mathbf{P}^e + \frac{(R_p\mathbf{s}_p + R_{se}^{en}\mathbf{P}^n + R_m\mathbf{s}_m - R_{tot}\mathbf{P}^e)}{Q(P^e)}$$

$$\frac{\partial \mathbf{P}^n}{\partial t} = \gamma^n(\mathbf{B}+\mathbf{B}_e)\times\mathbf{P}^n - \mathbf{\Omega}\times\mathbf{P}^n + R_{se}^{ne}(\mathbf{P}^e-\mathbf{P}^n) - R_{sd}^n\mathbf{P}^n, \tag{1}$$

where $\mathbf{P}^e$ and $\mathbf{P}^n$ are the polarizations of the electron spin and nuclear spin, respectively; R_p is the pumping rate of the electrons, R_{tot} is the total relaxation rate of the electrons, R_{se}^{en} and R_{se}^{ne} are the spin-exchange rate between the electrons and nuclei, respectively; R_p and R_m are the pumping rate of the pump-beam and probe-beam, respectively; and R_{sd}^n is the spin-destruction rate of the nuclei; $\mathbf{B}$ is the residual magnetic field, $\mathbf{B}_e$ and $\mathbf{B}_n$ are the magnetic fields generated by the electrons and nuclei, respectively; $\mathbf{L}$ is the light-shift generated by the electrons; $Q(P^e)$ is the nuclear slowing-down factor; γ^e and γ^n

978-1-5386-3758-6/18/$31.00 ©2018 IEEE

are the gyromagnetic ratios of the electrons and the nuclei, respectively.

By solving the Bloch equations in Eq. (1) with the transverse polarization P_x^e in steady state, we can obtain the following expression for a SERF ASG:

$$P_x^e = \frac{\gamma^e P_z^e R_{tot}^e}{{R_{tot}^e}^2 + (\gamma^e)^2 (L_z + \delta B_z - Q\Omega_z / \gamma^e)} \tilde{\Omega}_y , \tag{2}$$

where the longitudinal polarization of the electrons is $P_z^e = R_p / R_p + R_{rex}$. The output signal of the gyroscope is proportional to the rotation angle θ of the linearly polarized probe-beam, and can be given by

$$S_{ch1} = 2 I_0 A \theta \tag{3}$$

where

$$\theta = \frac{\pi}{6} l \cdot n \cdot r_e \cdot c \cdot P_x^e \cdot \{-\mathrm{Im}[\mathrm{V}(\nu - \nu_1)] + \mathrm{Im}[\mathrm{V}(\nu - \nu_2)]\} \tag{4}$$

Here l is the length of the vapor cell, n is the saturation vapor pressure density of the alkali atoms, c is the speed of light, ν_1 and ν_2 are the D_1 line and D_2 line of the alkali atom, respectively. Combining Eqs. (2)-(4), the simulation result for the relation between the pump-beam intensity P and the gyroscope output signal S_{ch1} is shown in Fig.1. The pump-beam intensity has an optimal point, and the fluctuation of the pump-beam intensity can cause the fluctuation of the output signal. Thus, it is significant to improve the stability of pump-beam intensity, so that the drift of the SERF ASG can be restrained. Meanwhile, the instability of probe-beam I_0 would directly cause the drift of the output signal which can be stabilized only when the probe-beam entering the vapor cell is stabilized.

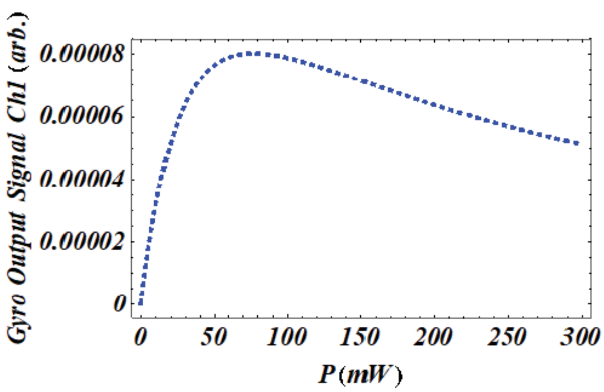

Fig.1. The gyro output signal varies with the pump-beam intensity

B. Operation principle

The basic composition of the optical path is shown in Fig. 2 with the azimuth of the fast axis. The light propagates along the z axis, and it is assumed that the laser beam becomes a linearly polarized light after passing through the isolators, and its azimuth is parallel to the z axis after passing through the half-wave plate. A LCVR is assembled between the half-wave plate and PBS, with its fast axis rotating 45° to the horizon. The PBS is one kind of polarizer, whose polarization stability is superior to average linear polarizers. The azimuth of the transmission axis for the linear polarizer (LP) is 45° and the modulation axis of the PEM is along the z axis. The azimuths of fast axis of the quarter-wave plate is parallel to the LP, and the azimuth of fast axis of the analyzer before the PD2 is perpendicular to the LP. The intensities of the two sub-beams, which is split by the NPBS, can be obtained from the Jones matrices. The Jones vector G_0 of the light passing through the half-wave plate can be written as

$$G_0 = E_0 \begin{bmatrix} 1 \\ 0 \end{bmatrix}, \tag{5}$$

where E_0 is the electric field amplitude and the incident light intensity is $I_0 = E_0^2$. The Jones matrix of the LCVR is

$$G_{LCVR}(\delta,\theta) = \begin{bmatrix} \cos\theta & -\sin\theta \\ \sin\theta & \cos\theta \end{bmatrix} \begin{bmatrix} e^{j\frac{\delta}{2}} & 0 \\ 0 & e^{-j\frac{\delta}{2}} \end{bmatrix} \begin{bmatrix} \cos\theta & \sin\theta \\ -\sin\theta & \cos\theta \end{bmatrix}, \tag{6}$$

where δ is the phase retardation of the LCVR, and the azimuth of its fast axis is $\theta = 45°$. The Jones matrix of the PEM with its modulation axis orienting at 0° is

$$G_{PEM} = \begin{bmatrix} \cos[\alpha_0 (\sin\omega t)/2] - i\sin[\alpha_0(\sin\omega t)/2] & 0 \\ 0 & \cos[\alpha_0(\sin\omega t)/2] + i\sin[\alpha_0(\sin\omega t)/2] \end{bmatrix}, \tag{7}$$

where α_0 is the modulation amplitude and ω is modulation frequency of the PEM. The NPBS has no effect on the polarization of the laser beam. So, the Jones matrices of a NPBS, whose splitting ratio of the transmitted light and reflected light is $b:a$, are given by

$$G_{NPBS1} = \mathrm{a} \begin{bmatrix} 1 & 0 \\ 0 & 1 \end{bmatrix}, \tag{8}$$

$$G_{NPBS2} = \mathrm{b} \begin{bmatrix} 1 & 0 \\ 0 & 1 \end{bmatrix}. \tag{9}$$

Combining Eqs. (5)-(9), Jones vectors G_1 and G_2 of the beams on PD1 and PD2 can be derived, respectively by

$$G_1 = G_{NPBS1} G_{QWP} G_{PEM} G_{LP} G_{PBS} G_{LCVR}(\delta,\theta) G_0 , \tag{10}$$

$$G_2 = G_{Analyzer} G_{NPBS2} G_{QWP} G_{PEM} G_{LP} G_{PBS} G_{LCVR}(\delta,\theta) G_0 . \tag{11}$$

The intensities I_1 and I_2 on PD1 and PD2 can be deduced by

$$I_1 = G_1^* G_1 = \frac{1}{8} a^2 {E_0}^2 (e^{i\delta} + e^{-i\delta} - 2) = \frac{1}{4} a^2 I_0 (\cos\delta - 1), \tag{12}$$

$$\begin{aligned} I_2 = G_2^* G_2 &= \frac{1}{8} b^2 {E_0}^2 (2 - e^{i\delta} - e^{-i\delta})(\sin(\alpha_0(\sin\omega t)/2))^2 \\ &= \frac{1}{8} b^2 I_0 (1 - \cos\delta)(1 - \cos(\alpha_0(\sin\omega t))) \end{aligned} . \tag{13}$$

Here, a small portion of laser-beam is detected by PD1 to feed voltage signal into an electronic control unit while the main laser-beam arrives in PD2. According to Eq. (12) and

Eq. (13), the intensity I_1 is independent of the PEM modulation, so it is feasible to obtain the feedback laser-beam after the PEM module.

The relationship between the phase retardation and the effective value for driving AC voltage is as follows [11]

$$\delta = \begin{cases} \delta_0 & (V \le V_c) \\ \delta_0\left[\dfrac{2}{e^{-(\frac{V-V_c}{V_0})^M}+e^{(\frac{V-V_c}{V_0})^M}}\right]^2 & (V > V_c) \end{cases}, \qquad (14)$$

where V_c is the threshold voltage for normal work, and V_c, V_0, M are positive constants, δ_0 is the maximum retardation of LCVR, whose maximum value is π for half-wave LCVRs. Thus, as the control voltage increases, retardation δ decreases monotonically from δ_0 to 0, and I_2 increases before it reaches half-wave.

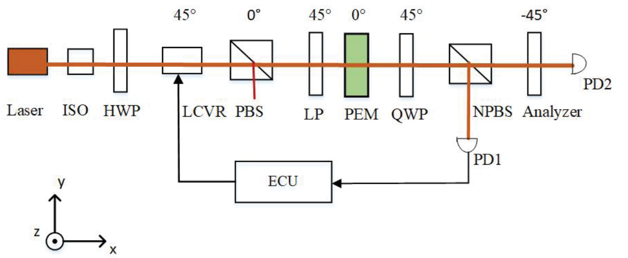

Fig.2. The light path of the probe-beam intensity stabilization control system. ISO: isolator, HWP: half-wave plate, PBS: polarization beam splitter, LP: linear polarization, QWP: quarter-wave plate, NPBS: nonpolarizing beam splitter, PD: photodiode.

III. Experimental Apparatus

Fig. 3 shows the diagram of the SERF ASG with the LCVR control system. Here a 10 mm diameter spherical vapor cell containing a mixture of K and Rb alkali metals, whose density ratio is about 1:100 at 180 ℃, 50 torr of N_2 gas and 2.3 amagat of ^{21}Ne gas, is used. The cell is placed in a heated oven with twisted-pair wires. The oven is enclosed by three cylindrical layers, which provide a shielding factor of 10^5 to quasi-static magnetic fields. Meanwhile, the residual magnetic fields could be further compensated by a set of three orthogonal Helmholtz coils outside the oven. The K-Rb hybrid pumping technique [12] is utilized in the gyroscope. A circularly polarized pump-beam whose wavelength is locked on the D1 line of K atoms polarized the K atoms directly. The Rb atoms are pumped by rapid spin-exchange collision with K atoms. Finally, the ^{21}Ne atoms are hyperpolarized by the Rb atoms by spin exchange. A Meadowlark Optics LVR-065 half-wave LCVR is used to stabilize the pump-beam intensity, so that the polarization of the atoms can be stabilized. A Glan-Prism (GL) is utilized as a beam splitter for the pump-beam intensity control, whose polarization stability is better than PBS. A small portion of pump-beam split by the GL is detected by PD, then the signal is transmitted into ECU. The embodiment of the ECU based on a STM32 mcu is shown in Fig.4. The feedback signal is acquired into the STM32 mcu through AD module, and the value of control voltage is calculated by a PID algorithm. Finally, the control voltage is used to control the phase retardation of the LCVR by DA module. The construction of the probe-beam sets forth as in Section 2, and the circuit control is identical to that for the pump-beam. Besides, the probe-beam is modulated by a PEM, which can reduce the 1/f noise in the rotation signal. The optical rotation signal detected by the photodiode can be demodulated by a digital lock-in amplifier and recorded by a computer.

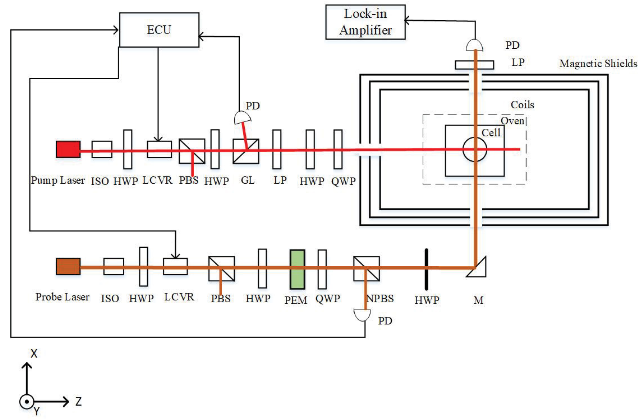

Fig.3. The diagram of the SERF ASG with the LCVR control system for pump-beam and probe-beam intensities. GL: Glan-Prism, M: mirror, ECU: electronic control unit.

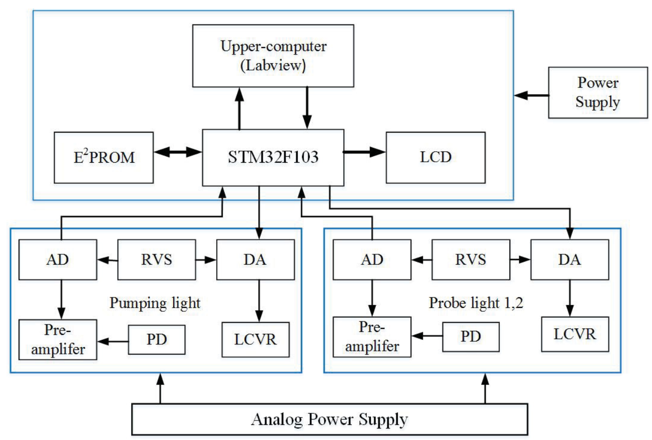

Fig.4. The block diagram of the electronic control unit.

IV. Experimental Results

The LCVR laser intensity control module has been used on a SERF ASG, whose diagram can be depicted in Fig. 3. The results for a 4-hour laser intensity test is taken and the representative performance of the probe-beam is shown in Fig. 5. Here, a standard deviation (STD) is applied to compare the output laser intensity under and without control. According to Fig. 5(b), the source laser intensity changes obviously without control because the controller of the source laser will vary with environment temperature, and its STD is about 0.64%. However, the combination of PEM module and LCVR laser intensity control module can significantly reduce the 1/f noise and improve the laser intensity stability. The test result is shown in Fig. 5(a) and its STD is about 0.0084% under control. The laser intensity under control is less affected by environment temperature, so that the stabilization of the spin polarization and background noise for the gyroscope can be optimized. The results of normalized output laser intensity under and without control is shown in Fig. 5(c), and it is obvious that this laser intensity stabilization control system is effective in restraining the laser drift with the varying environment temperature.

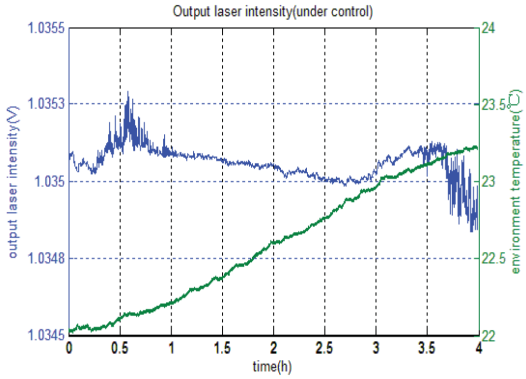

(a) Output laser intensity (under control)

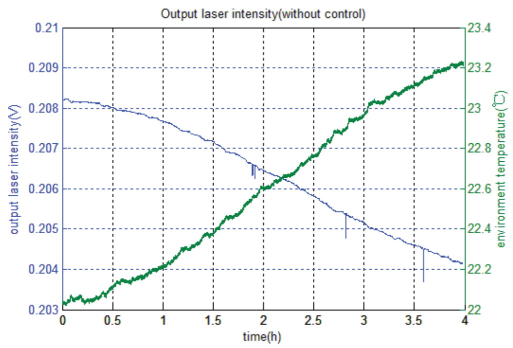

(b) Output laser intensity(without control)

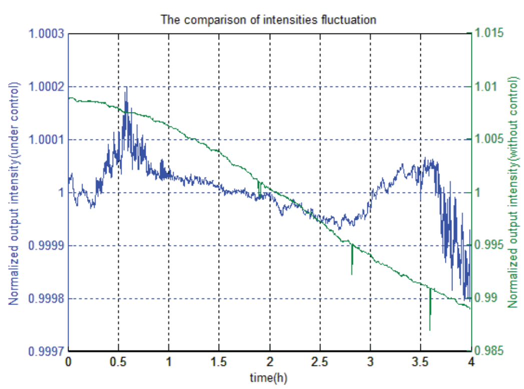

(c) the comparison of output laser intensities

Fig.5. The results for a 4-hour laser intensity test of the probe-beam. (a) output signal under control (blue line) and environment temperature (red line). The laser intensity is less affected by environment temperature. (b) output signal without control (blue line) and environment temperature (red line). The intensity varies with temperature obviously. (c) the comparison of normalized output intensity under control (blue line) and normalized output intensity without control (red line).

V. Conclusion

In conclusion, a LCVR based laser intensity stabilization control system combining a PEM module has been utilized to restrain the laser intensity fluctuations for a SERF atomic spin gyroscope. The stability of 0.0084% (the standard deviation) has been achieved in a 4-hour test, which is significantly better than the source laser-beam. Besides, the PBS or GL is used as a polarizer and light splitter, respectively, to improve the polarization stability of the optical path. Finally, the fact shows that our system can effectively reduce the fluctuation of laser-beam, and it is beneficial for improving the properties and miniaturization of atomic gyroscopes.

Acknowledgment

This work is supported by National High Technology Research and Development Program of China (863 Program), the National Natural Science Foundation of China (Grant Nos.61374210, 61673041 and 61227902), and the National Key R\&D Program of China (Grant No.2016YFB0501600).

References

[1] Barbour Neil, and George Schmidt. “Inertial sensor technology trends,” *IEEE Sensors journal*, 1(4) , pp.332-339, 2001.

[2] JianCheng Fang, and Jie Qin. “Advances in atomic gyroscopes: A view from inertial navigation a vol.pplications.” *Sensors*, vol. 12(5) , pp. 6331-6346, 2012.

[3] Kornack Thomas Whitmore, *A test of CPT and Lorentz symmetry using a K-3He co-magnetometer*. Ph.D. Thesis, Princeton University, 2005.

[4] Kornack T. W., R. K. Ghosh, and M. V. Romalis. “Nuclear spin gyroscope based on an atomic comagnetometer,” *Physical review letters* 95(23), pp. 230801, 2005.

[5] Li, Rujie, et al. “Rotation sensing using a K-Rb-Ne 21 comagnetometer,” *Physical Review A*, vol. 94(3), pp. 032109, 2016.

[6] Brown Justin Matthew. *A New Limit on Lorentz-and CPT-Violating Neutron Spin Interactions Using a Potassium-Helium Comagnetometer*. Ph.D. Thesis, Princeton University, 2011.

[7] Herke, Richard, Michael H. Anderson, and Thomas Baur. “Liquid crystals in precision optical devices,” *Liquid Crystals III*. vol. 3800. 1999.

[8] Jacobs, Stephen D., et al. “Liquid-crystal laser optics: design, fabrication, and performance,” JOSA B vol.5(9), pp. 1962-1979, 1988.

[9] Zeng, Aijun, et al. “Simultaneous measurement of retardance and fast axis angle of a quarter-wave plate using one photoelastic modulator,” *Applied optics*, vol.50(22), pp. 4347-4352, 2011.

[10] Vasilakis Georgios, *Precision measurements of spin interactions with high density atomic vapors*. Ph.D. Thesis, Princeton University, 2011.

[11] Liang, Qing, et al. “Laser intensity stabilization with a liquid crystal variable retarder for a nuclear magnetic resonance gyroscope prototype,” in *Applied Optics and Photonics China (AOPC2015)*. International Society for Optics and Photonics, 2015.

[12] Ito, Yosuke, et al. “Development of an optically pumped atomic magnetometer using a K-Rb hybrid cell and its application to magnetocardiography.” *AIP advances*, vol.2(3), pp.032127, 2012.